RESEARCH ARTICLE | JULY 01 1999

Vertical variant of a double channel-cut crystal spectrometer for investigation of laser-generated plasmas

O. Renner; P. K. Patel; J. S. Wark; E. Krousky; P. E. Young; R. W. Lee

Rev. Sci. Instrum. 70, 3025–3031 (1999)
https://doi.org/10.1063/1.1149863

Vertical variant of a double channel-cut crystal spectrometer for investigation of laser-generated plasmas

O. Renner
Institute of Physics, Academy of Sciences CR, 18221 Prague, Czech Republic

P. K. Patel and J. S. Wark
Department of Physics, Clarendon Laboratory, University of Oxford, Parks Road, Oxford OX1 3PU, United Kingdom

E. Krousky
Institute of Physics, Academy of Sciences CR, 18221 Prague, Czech Republic

P. E. Young and R. W. Lee
Lawrence Livermore National Laboratory, Livermore, California 94550

(Received 15 September 1998; accepted for publication 1 April 1999)

The theoretical design of multicrystal instruments which define a new class of spectrometers based on the vertical dispersion principle is reported together with experimental confirmation of design. Previous designs in the vertical-variant scheme—which have been fielded successfully in laser-produced plasma experiments—have operated with one or two crystal surfaces in a configuration that deflects the diffracted radiation back in the general direction of the source. The additional reflecting surfaces described here direct the radiation along a radial vector from the source to the detector, independent of the Bragg angle. Thus, the experimental setup is more flexible and greatly facilitates the coupling of the spectrometer to a charge-coupled device or streak camera. One of these instruments, a double channel-cut crystal spectrometer working in the vertical dispersion mode (DCCV), employs a total of four diffracting crystal surfaces. A compact design of the DCCV prototype is compatible with small bore reentrant diagnostic access tubes (e.g., the 6 in. manipulator) employed at several large-scale laser facilities. This high-dispersion spectrometer combines a high spectral resolution [$R=13\,500$ with Si(111) crystals] with a one-dimensional spatial resolution of the order of 20 μm. © *1999 American Institute of Physics.*
[S0034-6748(99)02707-0]

I. INTRODUCTION

X-ray spectroscopy has long been used as a means of diagnosing conditions of laser-produced plasmas, as information concerning both the temperature and density can be extracted from the emitted radiation. This subject area has been reviewed,[1] thus we will not emphasize the means by which such information is extracted from the recorded spectra. It suffices to say that x-ray spectroscopic instruments with a relatively wide spectral range (such as certain flat or convexly curved Bragg crystal spectrometers) are of particular use for deducing electron temperatures by measurement of the ratios of lines associated with different charge states. For these purposes, the spectral resolution of the x-ray spectrometer, whether intrinsic to the instrument itself or dictated by source broadening considerations, is not of paramount importance and can be quite modest, as it is the total radiation emitted over the line profile that is of import, rather than the detailed line shape. On the other hand, the inference of plasma density by the measurement of, for example, the width of a Stark-broadened line, obviously places a lower limit on the resolving power of the spectrometer. In addition to the requirement of spectral resolution, when shifts and alterations in the shape of spectral lines are also of interest (due, for example, to large velocity gradients within the plasma) the generation of a reference wavelength is also needed.

Over the past few years a group of relatively novel x-ray spectrometers based on the vertical dispersion principle[2,3] has aroused considerable interest for use in laser plasma experiments. The main attraction of the instruments is their capability to simultaneously achieve high spectral and spatial resolution supplemented by the production of two greatly dispersed spectra symmetrically disposed about a central wavelength. The spectral resolution of one of these instruments—the vertical variant of the double crystal x-ray spectrometer (DCV),[4] can in principle even exceed the single-crystal rocking curve limit over a limited spectral range. This spectral capability is combined with a spatial resolution at unit magnification of a few microns, dependent upon the rocking curve width and the total x-ray path length from source to detector. These features make the instrument ideal for low spectral range, high resolution measurements of single or small numbers of closely spaced lines.

The principle of the DCV was first suggested by Hrdy[5] in 1968, but its implementation in laser plasma investigations took more than two decades.[4,6] The ultrahigh resolution of the instrument used in these experiments, coupled with its ability to provide a stable relative wavelength reference, al-

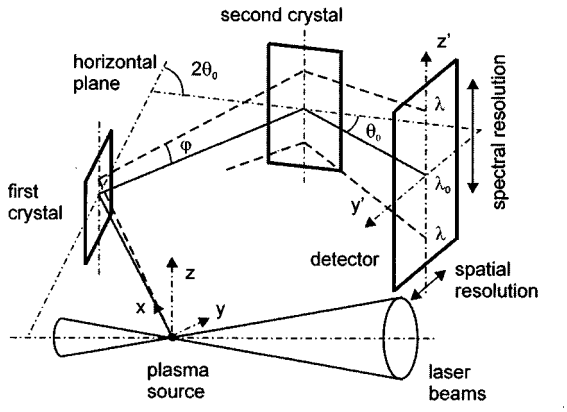

FIG. 1. Schematic diagram of the double crystal x-ray spectrometer.

lowed detailed measurements of the effects of velocity gradients on the $n=2-1$ transition in hydrogenic aluminum. After these experiments a detailed description of the theory and performance of the instrument was provided.[7]

However, despite the many advantages, there are practical limitations to the applicability of the DCV. The nature of these difficulties can be seen by referring to the schematic diagram of the DCV shown in Fig. 1. X rays from the source are diffracted from two single crystals. The central wavelength λ_0 about which the two symmetric spectra are disposed, is determined by the angle $2\theta_0$ between the two crystals. X rays at this central wavelength are coplanar with the normals to the two crystals, and lie in the horizontal plane as depicted in the diagram. The wavelengths shorter than λ_0 can also satisfy the Bragg diffraction condition on both of the crystals when their paths lie in the vertical planes containing the central ray and parallel to the intersection of the diffraction planes, the diffraction condition being

$$\lambda = \lambda_0 \cos \varphi, \tag{1}$$

where φ is the standard vertical divergence angle measured from the horizontal plane. This relation is the starting point for determination of the instrumental characteristics as laid out by Renner *et al.*[7]

It can be seen from Fig. 1 that, by its very design, the x rays take a dogleg path from source to film, that is to say the double reflection directs the x rays back in the general direction of the source. Furthermore, the precise path that the x rays take is dependent upon the angle between the two crystals (as this dictates the central wavelength). This characteristic of the DCV poses a number of difficulties. First, the instrument tends to take up a significant solid angle surrounding the x-ray source of interest, limiting the scope for the fielding of further diagnostics. Second, it limits the options for using alternative and perhaps larger detectors in place of film. This is particularly true for the case of coupling to a streak camera if a time resolved record of the x-ray emission is desired. A streak camera, because of its size and construction, is usually deployed along a radial vector, or direct line of sight, to the source, with its entrance slit in a fixed plane normal, or near-normal, to this line of sight. To couple to the DCV would require the detection plane of the DCV to be coincident with the entrance plane of the streak camera. Given the geometry of the DCV the practical difficulties of such an arrangement are considerable, and are furthermore exacerbated by the fact that the position of the detection plane must be changed with each angular setting of the crystals. While it may, by some judicial arrangement and design of chamber, be possible to overcome these limitations on smaller, flexible laser facilities, they remain severe obstacles to the deployment of the instrument on larger systems. In particular, several large laser facilities (such as the Nova Laser at Lawrence Livermore National Laboratory[8] and the Omega Laser at the University of Rochester[9]) require many of the target diagnostics to be deployed through reentrant vacuum-locked tubes (consistent with the so-called ''SIM-tubes'' where SIM stands for 6 in. manipulator[10]). These tubes are designed such that their axes lie on radial vectors from the target at the center of the vacuum chamber, and are thus unsuitable for deployment of the standard DCV, especially if coupling to a streak camera is the ultimate goal.

Thus, to overcome these difficulties, we have analyzed further variants of the DCV based on the diffraction of x rays from three or four crystal surfaces. One of these novel instruments, the recently developed double channel-cut crystal spectrometer working in the vertical dispersion mode (DCCV), is the main subject of this article. We first describe the principle of operation of the multicrystal configurations, along with calculations of their resolution (both spectral and spatial) and luminosity. We then describe preliminary experiments performed with the DCCV, and demonstrate that its measured response is consistent with that predicted.

II. SURVEY OF THE THEORY

The basic idea of the multicrystal configurations is to replace the first or both diffraction elements of the DCV by channel-cut crystals. These diffractors, which are commonly used at synchrotron sources, reflect x rays from the surfaces of the U-shaped grooves cut into blocks of single crystals. The relevant diffraction planes are aligned on an atomic scale, consequently the Bragg condition is satisfied at both inner surfaces simultaneously. Assuming symmetric diffraction and neglecting the narrowing of the rocking curve combined with a drop of transmitted intensity due to two reflections in a series, the channel-cut crystals disperse the radiation in the same manner as the single-reflection crystals. Thus a combination of the channel-cut and the single-crystal or two channel-cut crystals in nonparallel setting provides characteristics similar to the original DCV. The substantial difference consists in the direction of the transmitted radiation which is parallel with a beam incident onto each channel-cut crystal—the alteration of the ray paths is now moderated or suppressed.

The schemes of the novel high-resolution spectrometers are shown in Fig. 2. The channel-cut crystal in the configuration (a) diverts the diffracted radiation away from the source, the antiparallelly positioned single-crystal limits the horizontal divergence of the transmitted beam[7] and directs the rays to the detector. Although the solid angle subtended by the spectrometer is relatively small, the virtual source of

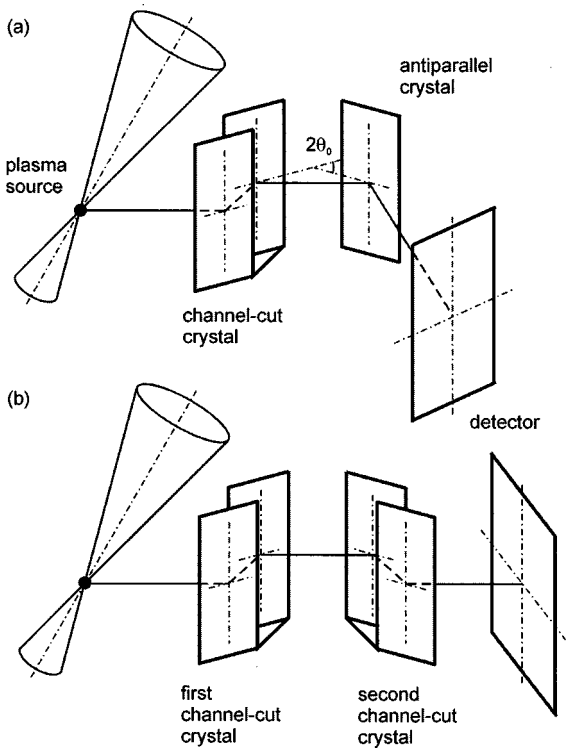

FIG. 2. Geometry of the (a) three- and (b) four-crystal configurations.

the x rays, as seen from the detector, still does not coincide with the position of the real source. Therefore, both major drawbacks of the DCV are eliminated in the second configuration of two channel-cut crystals which corresponds to the scheme of the DCCV. The lateral shifts of the beams transmitted at both diffractors are precisely compensated, thus the positions of the virtual and the real source overlap and do not depend on changes of the central wavelength λ_0.

The properties of the vertical-geometry instruments follow from a combination of the vertical dispersion principle and the integral equations describing the distribution of the power transmitted through the multicrystal spectrometers.[11] The differentiation of Eq. (1) provides directly the expressions for the angular dispersion

$$d\varphi/d\lambda = -1/(\lambda \tan \varphi), \tag{2}$$

and the linear dispersion

$$D_{\text{lin}} = \frac{dz'}{d\varphi}\frac{d\varphi}{d\lambda} = -L/(\lambda \cos\varphi \sin\varphi), \tag{3}$$

where L is the x-ray source to detector pathlength. The range of the wavelengths covered at a given span of φ is simply

$$\Delta\lambda = \lambda_0 - \lambda = \lambda_0(1-\cos\varphi). \tag{4}$$

The quantitative characteristics of the spectrometer were derived by using the modified Eq. (6) of Renner *et al.*[7] The irradiance P at the detector plane (y',z') can be written as

$$P(y',z') = \int_\lambda \int_y \int_z T(\alpha,\varphi,\lambda)H(\alpha)G(\varphi)S(y,z) \times J(\lambda-\lambda_0)C(\alpha,\varphi,\lambda)d\lambda\,dy\,dz, \tag{5}$$

where T is the overall transmission efficiency through protective foils, H and G the source intensity profiles in the horizontal and vertical directions, S the emission distribution in the source plane (y,z), and J the spectral composition of the emitted radiation. The horizontal and vertical divergence may be expressed as $\alpha = \tan^{-1}[(y'-y)/L]$ and $\varphi = \tan^{-1}[(z'-z)/L]$. The composite rocking curve C includes the effect of partial crossing of polarization vectors connected with the transfer of the radiation diffracted from the first dispersion element onto the antiparallel diffractor. The general form of this function is defined by

$$\begin{aligned} C(\alpha,\varphi,\lambda) = {} & I_\sigma(\lambda)[C_\sigma^\zeta(\gamma_{\text{I}})C_\sigma^\eta(\gamma_{\text{II}})\cos^2\epsilon \\ & + C_\sigma^\zeta(\gamma_{\text{I}})C_\pi^\eta(\gamma_{\text{II}})\sin^2\epsilon] \\ & + I_\pi(\lambda)[C_\pi^\zeta(\gamma_{\text{I}})C_\pi^\eta(\gamma_{\text{II}})\cos^2\epsilon \\ & + C_\pi^\zeta(\gamma_{\text{I}})C_\sigma^\eta(\gamma_{\text{II}})\sin^2\epsilon], \end{aligned} \tag{6}$$

where I_σ and I_π are the intensity fractions corresponding to the polarization components σ and π of the radiation incident on the first crystal, C_σ and C_π are the single crystal diffraction patterns of the relevant components given by the dynamical theory of diffraction, $\gamma_{\text{I,II}} = \pm\alpha - (1-\cos\varphi)\tan\theta_0 - (\lambda-\lambda_0)D_0$ are the angles of incidence of x rays onto the first and the second dispersion unit and $D_0 = \tan\theta_0/\lambda_0$ is the classic angular dispersion in the horizontal plane. The power exponents ζ and η are defined for the DCV by $\zeta = \eta = 1$, for the hybrid scheme of the channel cut and single crystal (HCV) by $\zeta = 2$ and $\eta = 1$, and for the DCCV by $\zeta = \eta = 2$. Finally the angle ϵ between the crossed electric-field vectors of the relevant polarization components follows from[12]

$$\epsilon = \cos^{-1}[1 - 2\sin^2\theta_0 \tan^2\varphi/(\cos^2\theta_0 + \tan^2\varphi)]. \tag{7}$$

Equations (3)–(7) represent a basis of ray tracing codes used to evaluate the characteristics of different experimental configurations, which are determined from the computed distribution of the transmitted power at the detector.[7] Independent of the spectral line shape (Lorentzian or Gaussian) and width, a unit radiance from 1 mm^2 of the source into a solid angle 1 mrad^2 is assumed. The spectral resolution $R = \lambda/\Delta\lambda$ is defined by the full width at half maximum (FWHM) value $\Delta\lambda$ corresponding to the monochromatic signal distribution. The luminosity B is simply the intensity maximum computed for the emission of an isolated spectral line. For illustrative purposes we shall represent the luminosity B in units of mrad^2, so that the real signal at the detector is obtained by multiplying B by the source radiance in units of $x/(\text{mrad}^2\,\text{mm}^2)$ where x stands for photons/s, J/s, or J. Vice versa, the source emission in the given spectral line can be easily computed from the signal measured. The spatial resolution in the direction perpendicular to the dispersion plane is determined by a point spread function, i.e., by the intensity distribution of a point source image; alternatively, it is the FWHM value of the composite rocking curve in the horizontal direction multiplied by the distance L.

The results of calculations using Eqs. (5)–(7) are presented in Figs. 3–5. Unless specified otherwise, the input parameters correspond to the following experimental setup:

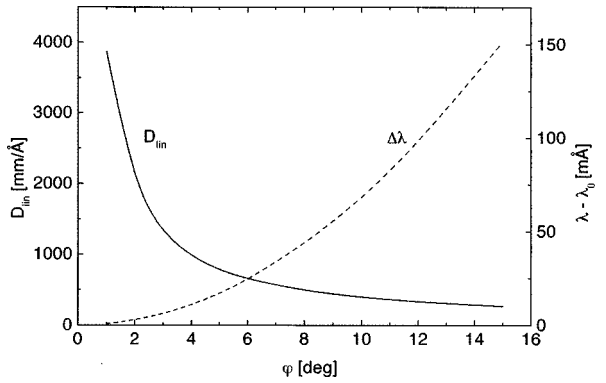

FIG. 3. The linear dispersion D_{lin} and the wavelength range $\Delta\lambda$ covered by the vertical-geometry schemes as a function of the angle φ.

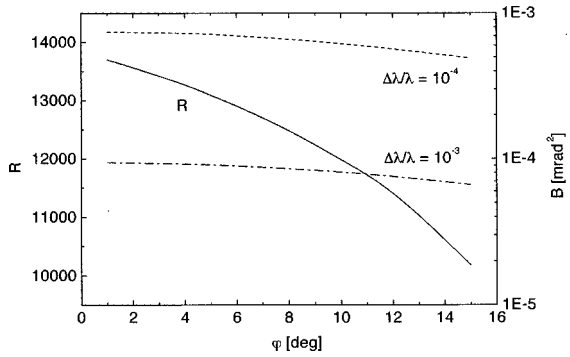

FIG. 5. Spectral resolution R and luminosity B of the DCCV as a function of the angle φ. The predicted intensity drop was calculated for two relative spectral linewidths $\Delta\lambda/\lambda$.

(1) The detection of the spectral line Cl He$\alpha[1s2p(^1P_1) \rightarrow 1s^2]$, at 4.4436 Å; (2) a symmetric Lorentzian profile with relative width $\Delta\lambda/\lambda = 1\times10^{-3}$; (3) Si (111) crystals with a refractive index-corrected interplanar spacing $2d = 6.2708$ Å; (4) a two-dimensional homogeneous, isotropic source of area $100\times100\ \mu$m squared; and (5) a source to detector distance $L = 300$ mm, with a vertical divergence angle $\varphi = 5°$—corresponding to $\theta_0 = 45.3445°$.

The characteristics plotted in Fig. 3 hold generally for all vertical-geometry schemes. The extremely high values of D_{lin} at low φ mostly compensate for the source-size induced apparatus smearing; for comparison, the linear dispersion of the Bragg single-crystal spectrometer (SC) is only 68.3 mm/Å at the same distance L. The wavelength range covered at different span of φ is rather limited but sufficient for a detailed investigation of isolated line profiles or narrow-band spectral features.

The spectral resolution and luminosity of the DCV, HCV, and DCCV are compared in Fig. 4. The resolution of the multicrystal configurations grows with L relatively rapidly at first and then gradually approaches the limiting value given by the width of the composite rocking curve. Except for the DCV resolution $R = 7800$ computed for $L = 100$ mm, the resolving power exceeds the ultimate value 7900 determined by the relevant single-crystal diffraction pattern.[13] As discussed previously,[7] this behavior corresponds to the narrowing of the composite rocking curve at repeated reflections from the crystals. With the same experimental conditions, the source size-limited resolution of the flat crystal spectrometer is reduced to $R = 1000-4500$ for $L = 100-500$ mm.

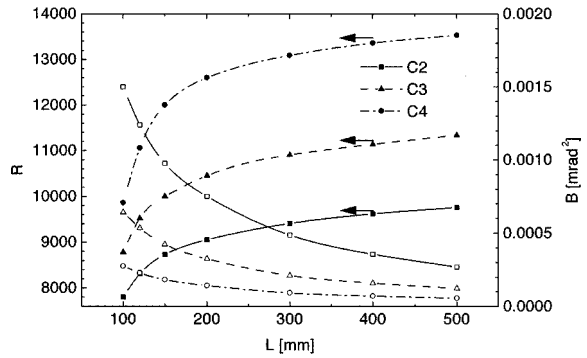

FIG. 4. Spectral resolution R and luminosity B of the two-, three-, and four-crystal configurations plotted as a function of the source to detector distance L.

The multicrystal schemes in general have low collection efficiencies, which decrease with growing L. For example, the collection efficiency of the DCV is more than one order of magnitude lower than that of the SC, while that of the DCCV is lower still by a further factor of 6. However, the situation improves when spatially resolved spectroscopic data are required. Due to the two-dimensional character of the composite rocking curve, spatial resolution is an intrinsic property of the multicrystal configurations. At $L = 300$ mm, its value for DCV, HCV, and DCCV is equal to 29, 23, and 18 μm, respectively. To achieve the same resolution, the Bragg spectrometer must include a horizontal slit of corresponding width, and then the luminosity of the SC is only a factor of 20 larger than that of the DCCV. On the other hand, the DCCV provides a spectral resolution of 13 000, considerably greater than the SC value of 3700.

Figure 5 demonstrates that the spectral resolution decreases markedly with increasing φ—at smaller values of linear dispersion, the effect of the source broadening is not fully negligible but still the resolving power remains well above the ultimate diffraction limit of the single crystal. The relatively slow intensity drop due to partial crossing of polarization vectors is not critical but should be taken into account at higher angles φ. As a practical consideration, the maximum value of φ is not limited solely by the size of the crystals and the effective area of the detector but also by the gradual loss of spectral resolution and transmitted power.

The reconstruction of the detected spectra is relatively simple. Assuming that the values of λ_0 and L are known, the intensity distribution in the detector plane (y',z') can be easily recalculated for the wavelength scale by means of Eq. (1). The precision in the absolute and relative wavelength determinations has been analyzed for the DCV in previous papers;[4,7] those conclusions generally hold for all of the multicrystal configurations described here. The computer-simulated experiments suggest that in most cases, the apparatus smearing function is negligible and the measured spectral profiles do not require deconvolution. In spite of this, the design of every concrete experiment ought to be accompanied by a detailed ray tracing analysis which pro-

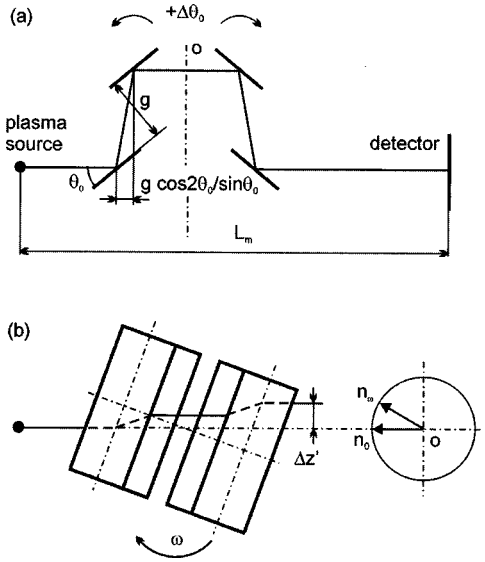

FIG. 6. Ray trajectory in the horizontal plane (a) and the vertical displacement of the transmitted beam $\Delta z'$ at cradled crystal position (b) due to rotation of the diffraction plane normals by angle ω around the axis o.

vides a fast and efficient tool to confirm the instrumental parameters expected.

III. DESIGN AND PERFORMANCE OF THE DCCV

The principal characteristics of the DCCV and the interplay between them have been outlined in the preceding section. The final design of the instrument starts from these parameters and additionally respects the constraints introduced by actual experimental conditions, particularly maximum outer dimensions determined by the target chamber configuration, required tunability of the spectrometer to different Bragg angles, and compatibility with advanced detection systems.

The prototype of the spectrometer fulfills the requirements imposed by the SIM geometry of the Nova laser. The scheme finally adopted utilizes two silicon channel-cut crystals with outer dimension $58\times19\times19\,\mathrm{mm}^3$ and active inner reflecting areas $50\times11\,\mathrm{mm}^2$ (vertical–horizontal direction) separated by a groove of width $g=5$ mm [see Fig. 6(a)]. The diffraction planes (111) are parallel to the precisely oriented mirror-reflecting outer surfaces of the crystal blocks. The reflection properties of the active surfaces were checked on a double crystal diffractometer by measuring the rocking curves corresponding to the Cu $K\alpha$ radiation generated by a standard x-ray tube. The measured FWHM widths were only 10%–19% larger, and reflectivities 6%–10% smaller, than predicted theoretical values. This close correspondence indicates that the reflection characteristics of the crystals are in near-perfect accordance with the dynamical theory of x-ray diffraction.

The range of the central Bragg angles (30.7°–46.0°) covered at different angular settings of the crystals [the value of θ_0 changes by rotating the crystal blocks in opposite directions about their vertical axis, as indicated in Fig. 6(a)] corresponds to the wavelength range 3.2–4.5 Å. This wavelength coverage can be modified by replacing the Si(111) crystals with diffractors having an alternative interplanar spacing.

Assuming a minimum distance between the entrance slit and the source of 100 mm, the vertical divergence of the beam accepted by the instrument is limited to about ±6° with respect to the horizontal plane of symmetry. The limited wavelength range of the two identical spectra corresponding to this span of φ is ideal for the identification of small spectral shifts or a detailed investigation of isolated line profiles. An operating mode providing a larger wavelength coverage in one of these spectra can be realized with an off-symmetric operation, which extends the field of possible applications considerably.

To achieve off-symmetric operation, both crystal blocks are mounted upon a cradle pivoting around the horizontal axis of symmetry ''o'' of the active crystal surfaces (see Fig. 6). By altering the tilt of the cradle ω, the vertical divergence of the beam transmitted through the DCCV in the upper and lower half-plane varies. The positive (clockwise) rotation increases the maximum value of φ in the upper half-plane but simultaneously decreases the fractional wavelength coverage in the lower one. For instance, at $\omega=7.5°$ the φ range is $\{-0.3°, +12.6°\}$; the wavelength coverage in the upper spectrum exceeds 77 mÅ for $\lambda_0=3.2$ Å (i.e., $\Delta\lambda/\lambda_0=2.4\times10^{-2}$), as compared to 0.05 mÅ in the lower one. These results assume a detector height of at least 67 mm. If coupled to a standard streak camera with a cathode length 20 mm positioned close to the spectrometer axis, the largest fractional wavelength coverage is $\Delta\lambda/\lambda_0=8.6\times10^{-3}$.

Furthermore, the tilt of the cradle introduces an asymmetry into the wavelength range covered by both spectra, changes the linear dispersion according to Eq. (3), and tunes the wavelength detected in a given distance z' above the horizontal plane. The detailed explanation of these effects follows from analysis of the cradled DCCV geometry. As indicated in Fig. 6, the difference ΔL between the straight source to detector distance L_m and the distance measured via the crystals L is

$$\Delta L = L - L_m = 4g \sin\theta_0 . \tag{8}$$

The angular displacement of the cradle ω corresponds to rotation of the diffraction plane normals n from the original horizontal plane to a new direction n_ω, thus the exiting rays are parallel to the incoming ones but vertically shifted. The displacement $\Delta z'$ of the horizontal beam[12]

$$\Delta z' = \Delta L \tan\omega \tag{9}$$

introduces a small correction to the wavelength scale. Assuming that the plane of detection is vertical, the divergence $\varphi_{z'}$ of the ray registered with the spatial coordinate z' is given by

$$\varphi_{z'} = \omega + \tan^{-1}[(z' - \Delta z')/L_\omega], \tag{10}$$

where $L_\omega = L_m + \Delta L/\cos\omega$. This relation is used to reconstruct the spectra—the wavelengths follow from Eq. (1), λ_0 is defined by the aligned angular position θ_0 of the crystal blocks, or by identifying lines in the detected spectra with their tabulated values.

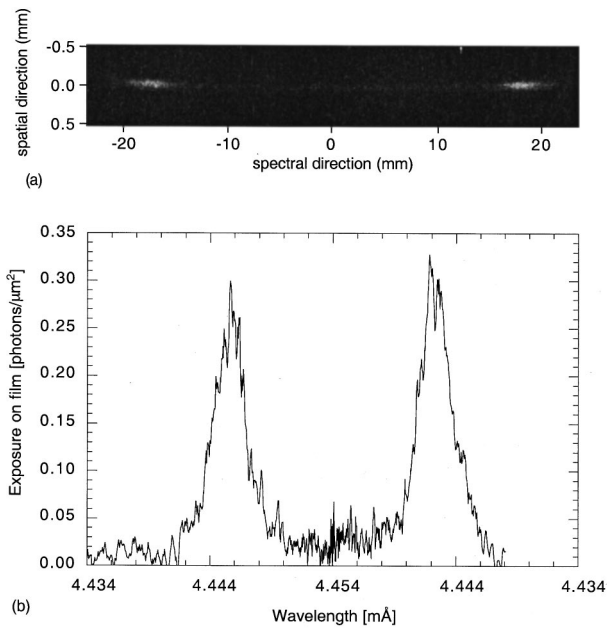

FIG. 7. The densitometer scan of the He-like Cl resonance line recorded with the DCCV (a), and its reconstruction to the wavelength scale (b).

IV. EXPERIMENT

The prototype of the DCCV was tested on the Janus Laser Facility at Lawrence Livermore National Laboratory. A single beam containing 40 J of 0.53 μm light in a 1-ns-square pulse was focused onto a saran (polyvinylidenechloride) target in a 30-μm-diameter focal spot, generating a peak irradiance of $5\times10^{15}\,\mathrm{W/cm^2}$. The plasma was observed at 45° to the laser axis. Its size and radiative emission were monitored by a pinhole camera and a survey spectrometer with a flat crystal of KAP. The resonance line of He-like Cl($\lambda=4.4436\,$Å) could be detected in a single shot, at a vertical divergence angle of 3.5° with a source-to-crystals-to-detector distance of 291.2 mm, on to Kodak DEF x-ray film.

The alignment procedure of the DCCV is fast and efficient; it requires an auxiliary He–Ne laser and a vertical-axis rotation stage. First, in the cradle position $\omega=0$, the normals to the diffraction planes (their orientation against the mirror-polished outer surface of the crystal blocks was known with a precision better than 10 arcsec) were aligned horizontal and perpendicular to a reference plane by autocollimation with the laser. The required angular position of the active crystal surfaces was fixed by rotating the whole spectrometer by the angle θ_0 and turning the crystal blocks around their individual vertical axes until the backreflected laser beams coincided with a circular aperture defining their diameter. Finally the cradle was tilted to the desired position ω.

The effective size of the hard x-ray emitting region of the plasma was estimated at $75\times75\,\mu\mathrm{m}^2$—somewhat larger than the focal spot size due to the expansion of the plasma. Figure 7(a) shows the spectrum recorded with the DCCV by integrating the signal over seven shots, corresponding to a total laser energy of 266 J. The horizontal axis in this image corresponds to the vertical dispersion direction of the spectrometer. This figure illustrates one of the unique characteristics of the vertical dispersion instruments, that is the production of two sets of spectra symmetrically placed about a central plane. The feature extending approximately 15–20 mm on either side of the center is the Cl Heα line. A 10-μm-wide spectral lineout from this image is plotted in Fig. 7(b). The distance on film has been calibrated to wavelength using Eq. (1) and the value $\lambda_0=4.4544\,$Å from the angular setting θ_0 of the crystals. Note that the single line either side of the central wavelength is due solely to Cl Heα resonance line emission, as the intercombination line at $\lambda=4.4669\,$Å and the associated Li-like satellite lines lie outside the spectral window of the instrument at this setting. Due to optical depth and velocity gradient effects, the FWHM of the observed resonance line $\Delta\lambda/\lambda=7.1\times10^{-4}$ is larger than the theoretical limit for the spectral resolution predicted by ray-tracing calculations ($\Delta\lambda/\lambda=7.4\times10^{-5}$); the conclusive measurement of the DCCV resolving power would require detection of spectra with well-defined fine spectral features.

To check the luminosity we can use the fact that x-ray sources of the Cl Heα type have been used for flash radiography of laser-fusion targets and their radiative characteristics are well known.[14] The conversion efficiency of the laser light into the Cl Heα line can, at the given conditions of energy deposition, be estimated at 3×10^{12} photons/(J 4π). Accordingly, the corresponding integrated plasma radiance is 1.13×10^4 photons/(mrad^2 μm^2). The expected exposure at the detector is obtained by multiplying the instrument luminosity $B=1.01\times10^{-4}\,\mathrm{mrad^2}$ by the source radiance. By assuming ideal diffraction from the crystals, this corresponds to a detected signal maximum 1.14 photons/μm^2. Taking into account the absorption in protective foils (25 μm Be, 12 μm mylar, and 0.4 μm Al) and the real reflectivity of the crystals we arrive at 0.50 photons/μm^2, which compares favorably with the maximum exposure 0.30 photons/μm^2 observed at the spectral line peak.

The spatial resolution in the direction perpendicular to the dispersion plane (ray tracing calculations predict a resolution of 18 μm) was verified indirectly by observing the plasma emission with a fine grid inserted between the source and the first crystal. The purpose of the grid was to effectively modulate the source intensity distribution in the horizontal direction, in which the 1D spatial resolution was obtained. The corresponding modulation in the signal distribution on the film introduced by a bar of thickness 50 μm is shown in Fig. 8. The theoretical profile has again been computed by assuming a homogeneous distribution of the source radiance which is a rather crude approximation. However, the reasonably good fit of the experimental and theoretical data indicates that the predicted spatial resolution of the DCCV is realistic.

V. DISCUSSION

The multicrystal configurations described in this article extend the field of applications of spectrometers based on the vertical dispersion principle, facilitating their coupling to sophisticated detection systems (e.g., charge-coupled devices, streak cameras), and supporting their compatibility with the standard geometries employed at large laser facilities.

In addition to the well-known characteristics of this type

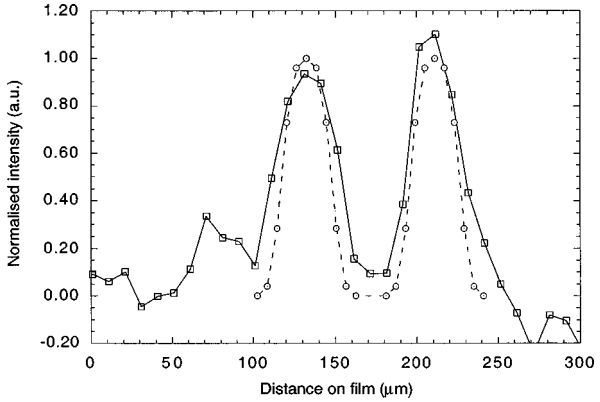

FIG. 8. Spatial lineout across the spectral line modulated by a 50 μm grid in front of the target. The fit of experimental (solid curve) and theoretical data (dashed) confirms the spatial resolution of the DCCV.

of instrument, i.e., extremely high dispersion, combination of spectral and spatial resolution, simultaneous production of two mirror-symmetric spectra, the channel-cut diffractors increase the ultimate resolution of the spectrometers, reduce the background due to fluorescence/scattering of radiation at crystals, and efficiently block direct irradiation of the detector. Although the wavelength range and the luminosity of the parallel-detecting, multicrystal schemes are small, the relative precision of the wavelength determination guaranteed by high-quality, well-characterized crystals may easily achieve 1×10^{-4} and 1×10^{-5} for absolute and relative measurements, respectively.[7]

The design of the DCCV and evaluation of its characteristics, as laid out here, indicate that the spectrometer is compact and easy to align. Finally, comparison of the main predicted and experimentally observed characteristics verifies the theory we have developed. The precise, absolutely calibrated multicrystal spectrometers are particularly suitable for investigation of profiles and positions of narrow-band spectral features or isolated spectral lines emitted from bright laser-produced plasmas.

ACKNOWLEDGMENTS

The authors gratefully acknowledge the assistance of the technical staff of the Janus Laser Facility, Lawrence Livermore National Laboratory. This work was supported by the Grant Agency of the Czech Republic under Grant No. 202/97/1186. One of the authors (P.K.P.) would like to acknowledge funding from the UK Engineering and Physical Sciences Research Council.

[1] A. Hauer, N. D. Delamater, and Z. M. Koenig, Laser Part. Beams **9**, 3 (1991), and references therein.
[2] O. Renner, M. Kopeck, E. Krousk, E. Förster, T. Missalla, and J. S. Wark, Laser Part. Beams **12**, 539 (1994).
[3] O. Renner, T. Missalla, and E. Förster, Proc. SPIE **2523**, 155 (1995).
[4] H. He, J. S. Wark, E. Förster, I. Uschmann, O. Renner, M. Kopeck, and W. Blyth, Rev. Sci. Instrum. **64**, 26 (1993).
[5] J. Hrd, Czech. J. Phys., Sect. B **18**, 532 (1968).
[6] J. S. Wark, A. Djaoui, S. J. Rose, H. He, O. Renner, T. Missalla, and E. Förster, Phys. Rev. Lett. **72**, 1826 (1994).
[7] O. Renner, M. Kopeck, J. S. Wark, H. He, and E. Förster, Rev. Sci. Instrum. **66**, 3234 (1995).
[8] E. M. Campbell, Laser Part. Beams **9**, 209 (1991).
[9] T. R. Boehly, D. L. Brown, R. S. Craxton, and R. L. Keck, Opt. Commun. **133**, 495 (1997).
[10] J. D. Kilkenny, Rev. Sci. Instrum. **63**, 4688 (1992).
[11] J. Drahokoupil and A. Fingerland, in *Advances in X-ray Spectroscopy*, edited by C. Bonnelle and C. Mandé (Pergamon, Oxford, 1982), p. 167.
[12] J. Hrd, Czech. J. Phys., Sect. B **35**, 401 (1985).
[13] G. Hölzer, O. Wehrhan, and E. Förster, Cryst. Res. Technol. **33**, 555 (1998).
[14] D. W. Phillion and C. J. Hailey, Phys. Rev. A **34**, 4886 (1986).